Radiometric Cross-Calibration of GF-4/IRS Based on MODIS Measurements

Xiang Zhou, Duo Feng, Yong Xie, Zui Tao, Tingting Lv, and Jin Wang

***Abstract*—GaoFen-4 (GF-4) infrared spectrum (IRS) camera has a special spectral band located in the mid-wave infrared spectrum with the wavelength ranging from 3.50 to 4.10 μm. It is very important for forest fire-detection and other quantitative remote sensing applications at a high spatial resolution of 400 m. Due to the similarity of the spectral characteristics, the thermal emissive band 20 (3.660–3.840 μm) and 22 (3.929–3.989 μm) of medium resolution imaging spectrometer (MODIS) are taken as the reference bands for the radiometric cross-calibration of the GF-4/IRS camera. The time difference between selected GF-4/IRS and MODIS images at the Qinghai Lake and Se lincuo Lake test sites is less than one hour. After spatial matching, single-band and dual-band spectral matching methods are proposed in this article. Then, the DN value of GF-4 image is linearly fitted to the radiance of the corresponding MODIS image to obtain the radiometric calibration coefficients of GF-4/IRS camera. The validation results show that the cross-calibration coefficients calculated by integrating the measurement of two MODIS bands with the mean value spectral matching approach has the highest radiometric calibration consistency with the official calibration coefficients.**

***Index Terms*—Dual-band method, GaoFen-4 (GF-4), infrared spectrum (IRS), medium resolution imaging spectrometer (MODIS), radiometric cross-calibration.**

I. Introduction

GAOFEN-4 (GF-4) is the only geostationary remote sensing satellite in China's high-resolution Earth Observation System, which was successfully launched on December 29, 2015 [1]. The payloads of GF-4 include both a panchromatic and multispectral (PMS) camera with the spatial resolution of 50 m and an Infrared spectrum (IRS) camera with the spatial resolution of 400 m [2]. Since GF-4 operates in a geosynchronous orbit, it can measure the Earth surface with a higher temporal resolution than a sun-synchronous orbit satellite. The width of each GF-4 image can be up to 400 km [3]. Due to its high spatial and temporal resolution and wide image coverage, GF-4 images are widely used in many application fields, such as disaster reduction and relief, ecological environment monitoring, target tracking and so on. GF-4/IRS is a camera with a special band located in the mid-wave infrared spectrum, originally designed for forest fire monitoring. The wavelength of this special band is from 3.50 to 4.10 μm with the center wavelength of 3.80 μm [3].

Radiometric characterization of remote sensor will change with the time it travels in space. Therefore, timely on-orbit radiometric calibration of sensors is very important to ensure the accuracy of quantitative remote sensing applications. At this stage, three typical methods are usually used for on-orbit radiometric calibration of satellite sensors, such as site calibration, on-board calibrator and cross-calibration method. However, since no on-board calibrator was designed and installed, the radiometric calibration of the PMS and IRS cameras of the GF-4 satellite was performed only once per year through the site calibration method, because this is a time-consuming and laborious task and is extremely vulnerable to weather. Due to limited calibration frequency, it is difficult to eliminate random errors and to track the radiometric stability of GF-4/IRS sensor. Thus, we can achieve more frequent radiometric calibration coefficients of GF-4/IRS through cross-calibration and track the radiometric consistency in its mission lifetime.

Cross-calibration is an alternative way to acquire the radiometric coefficient of the remote sensor. It uses a well-calibrated sensor as a reference and compares the radiometric response of two sensors over the same target within a small imaging time difference. Teillet *et al.* used the Landsat-5 and SPOT HRV images acquired on the same day to scale NOAA-9 and NOAA-10 AVHRR based on the White Sand Test Site in New Mexico, USA [4]. Calibration coefficients of three remote sensors, AVHRR, SeaWiFS and Vegetation, were obtained with time series cross-calibration by taking POLDER as the reference and choosing North Africa and Saudi Arabia as research areas [5]. Chander *et al.* analyzed SCIAMACHY hyperspectral data using Envisat satellite. At the same time, he also used EO-1 satellite Hyperion hyperspectral data to obtain spectral band adjustment factor, and found that the former can improve cross calibration accuracy better than the latter [6]. Thome *et al.* selected ETM+ as a reference remote sensor to cross-calibrate Hyperion, Terra/ medium resolution imaging spectrometer (MODIS), and IKONOS based on the Railroad test site [7]. Moeller compared the simulated MODIS radiances with the MODIS observations, results of which show that Aqua MODIS TIR bands are performing well. The residuals (MAS—MODIS) in most bands are within or very close to the specifications. The residuals of

Manuscript received May 24, 2021; revised June 4, 2021 and June 15, 2021; accepted June 20, 2021. Date of publication June 23, 2021; date of current version July 15, 2021. This work was supported in part by the Joint Validation of Multi-source Remote Sensing Information and Sharing in BRICS Countries under Grant 2018YFE0124200, and in part by Land Observation Satellite Supporting Platform of National Civil Space Infrastructure Project. *(Corresponding authors: Zui Tao; Tingting Lv.)*

Xiang Zhou, Zui Tao, Tingting Lv, and Jin Wang are with the Aerospace Information Research Institute, Chinese Academy of Sciences, Beijing 100101, China (e-mail: zhouxiang@radi.ac.cn; taozui8421@163.com; lvtt@radi.ac.cn; wangjin@aircas.ac.cn).

Duo Feng and Yong Xie are with the School of Geography and Remote Sensing, Nanjing University of Information Science and Technology, Nanjing 210044, China (e-mail: 20171389005@nuist.edu.cn; xieyong@nuist.edu.cn).

Digital Object Identifier 10.1109/JSTARS.2021.3091977

split window (band 11 and 12 μm) are small and very close to one another (at $-0.15\,^{\circ}$C and $-0.13\,^{\circ}$C, respectively) [8]. Based on this research, Xie *et al.* proposed that the near-simultaneous observations from MODIS and atmospheric infrared sounder (AIRS) sensors on-board the Aqua spacecraft provide a good opportunity to track the relative calibration stability of both sensors over their entire mission. The trend results show that the brightness temperature difference of all the MODIS bands that can be calculated has a change of less than 0.3 K in 6 years, and is slightly larger at large scan angles than those near nadir [9]. Wu *et al.* research compared the calibration differences between the Aqua MODIS and NOAA-18 AVHRR bands centered at 11.0 and 12.0 μm using simultaneous nadir overpass observations obtained in nearly parallel orbits. Results indicated an excellent calibration consistency between MODIS and AVHRR for both bands [10].

Before the launch of GF-4, only Huanjing-1B (HJ-1B) in HJ satellite constellation in China terrestrial observation system has a thermal infrared band whose center wavelength of about 11 μm. Liu *et al.* used AIRS hyperspectral measurements to perform multi-point cross-calibration and verification of HJ-1B thermal infrared channel. By eliminating the abnormal points in the time series, using multipoint method and adjusting the matching factors in the uniform target multipoint method, the calibration results obtained by the experiment are accurate and credible [11]. Yang *et al.* used MODIS to calibrate the thermal infrared channel of HJ-1B, compared and analyzed observation angles and imaging time difference to obtain higher calibration accuracy [12]. On the basis of the calibration of the thermal infrared radiometer CE312, Liu *et al.* used CE312 to perform on-orbit radiometric calibration of the thermal infrared channel onboard HJ-1B satellite. The experimental results showed that the accuracy of the calibration coefficient obtained by the two-point method is higher than that of the single point method [13]. However, this satellite no longer provides observation service. Therefore, GF-4/ IRS is the only on-orbit sensor with mid-wave infrared band for terrestrial observation. To our best knowledge, there are few researches on cross-radiation calibration of GF-4/IRS sensor.

In this article, MODIS, a multiband remote sensor with high radiometric calibration accuracy, is selected as the reference sensor to cross-calibrate the GF-4/IRS sensor. In order to obtain calibration coefficients with high precision, five spectral matching methods with single-band or dual-band measurement are proposed, and the radiometric discrepancy caused by spectral differences between two sensors is fully considered. Comparative analysis of the calibration results derived from five methods confirmed that the calibration coefficients obtained by the dual-band method with the mean value approach are more accurate and reliable.

The organization of this article is as follows: reference sensor, the test sites and datasets are described in Section II. Section III introduces the basic principle of cross-calibration, and detailed spatial and spectral matching methods. Results of radiometric calibration are illustrated in Section IV. Finally, Section V concludes the article.

II. Reference Sensor, Test Sites, and Datasets

Before the calculation of calibration coefficients, the basic preprocessing process must be performed first, including three important steps.

1) *Step* 1: Choose a reference sensor which is suitable for cross-calibrating GF-4/IRS.
2) *Step* 2: Looking for an ideal place as our test site.
3) *Step* 3: Search for simultaneous images over test site for both sensors.

A. Selection of Reference Sensor

According to the theory of cross-calibration, we select MODIS as the reference sensor to calibrate the GF-4/IRS because the radiometric calibration accuracy of MODIS is quite outstanding and frequently used as reference sensor. MODIS can update the calibration coefficients every two months by using various calibration techniques such as on-board calibration and cross-calibration techniques. In the emergency situation, the higher frequency can be realized to ensure the quality and stability of the remote sensing measurements. The radiometric resolution is up to 12 bits, and the radiometric calibration error in the thermal infrared band is controlled within 1 K, and the optimal is 0.5 K [9]. Zhang *et al.* used the MODIS satellite observation to evaluate and analyze the accuracy of the radiometric calibration method for the thermal infrared channel of the Chinese remote sensing satellite. The results showed that the calibration accuracy of the hot infrared window channel is better than 1.0 K [14].

MODIS is a key instrument designed for the study of atmosphere, land, ocean, etc., [15]. Two MODIS sensors are operating onboard both Terra and Aqua spacecrafts, respectively, and are circling around the Earth in a polar sun-synchronous orbit at the height of 705 km. Since Terra and Aqua are near-polar sun-synchronous orbit satellites, the former transits at 11:30 a.m. local time for observation, and the latter transits at 1:30 p.m. local time. MODIS is a cross-track scanning radiometer with a two-side scan mirror which rotates within a scan angle range of $\pm 55^{\circ}$ for Earth observations, corresponding to a 2330 km-wide-swath at the surface. Therefore, by integrating measurements from two MODIS sensors with different local transit times, we can double the chance of obtaining the simultaneous measurement pairs. MODIS has 36 spectral bands, including 20 reflective solar bands and 16 thermal emissive bands, to conduct the Earth observations within the spectral range from 0.4 to 14.2 μm. Band 20 (3.75 μm) and 22 (3.97 μm) are two bands whose wavelength ranges are very close to GF-4/IRS. Moreover, the spatial resolution of MODIS thermal infrared band is 1000 m and that of GF-4/IRS is 400 m, which is suitable for spatial match. Therefore, we select MODIS as reference sensor for calibrating GF-4/IRS.

B. Test Site

For the selection of GF-4 and MODIS measurements, two following conditions must be met. First, both GF-4/IRS and MODIS observe the same test site. Second, considering that the

Fig. 1. RGB true color images of GF-4/PMS over Qinghai Lake (left) and Se Lincuo Lake (right).

TABLE I
DETAILED INFORMATION OF THREE IMAGE PAIRS

Test site	Date	GF-4/IRS imaging time (UTC)	MODIS imaging time (UTC)	Number of calibration points
Qinghai Lake	2016.05.10	6:45 a.m.	6:40 a.m.	75
Se Lincuo	2016.05.11	7:01 p.m.	7:20 p.m.	76
	2016.05.14	5:13 p.m.	4:40 p.m.	75

atmospheric conditions will not change too much to affect the radiometric response, the transit time between the two sensors is usually less than 1 h [16]. In our research, we chose Qinghai Lake and Se Lincuo Lake as the radiometric calibration area because the water body has a larger specific heat capacity and will not change significantly in a short period of time. The red, green, and blue (RGB) true color images of GF-4/PMS over Qinghai Lake and Se Lincuo Lake are shown in Fig. 1.

C. Datasets Selection

The images we used in this article were taken over Qinghai Lake on May 10, 2016 and over Se Lincuo Lake on May 11 and 14, 2016. Three image pairs are uncontaminated by either cloud clusters or snow. The difference in transit time of these image pairs is less than one hour, which meets the cross-calibration requirements. The detailed information of three image pairs is given in Table I. Meanwhile, the number of valid calibration points extracted from the corresponding image pairs with our spatial matching method is also given in Table I.

III. METHODOLOGY

A. Principle of Cross-Calibration of GF-4/IRS With MODIS

Principle of cross-sensor radiometric calibration is to calculate the calibration coefficient of an uncalibrated sensor by comparing simultaneous measurements with those from a well-calibrated sensor. That is, a relationship is established between the outputs of the two sensors to obtain calibration coefficients. In the process of our cross-calibration method, spatial match and spectral match are two critical steps to decide the accuracy of calibration coefficients. The flowchart of the cross-calibration process is drawn in Fig. 2.

B. Spatial Match

In order to achieve a good correlation between GF-4/IRS and MODIS, spatial match between image pairs should be preprocessed. The initial spatial resolution of the GF-4 thermal infrared band is 400 m, while the spatial resolution of the reference remote sensor MODIS is 1000 m. The spatial resolution needs to be unified to perform comparison. The spatial scale of GF-4 thermal infrared image, therefore, is converted to 1000 m by cubic convolution to match the MODIS image [17].

Then, the sliding windows (5×5pixels) are selected to extract the calibration points from the resampled GF-4/IRS image and MODIS image. Since the valid calibration points should be the homogeneous surface, the coefficients of variation (CV) (the radio of standard deviation and mean reflectance) of the sliding windows on image pairs are both lower than 3% in the article [18].

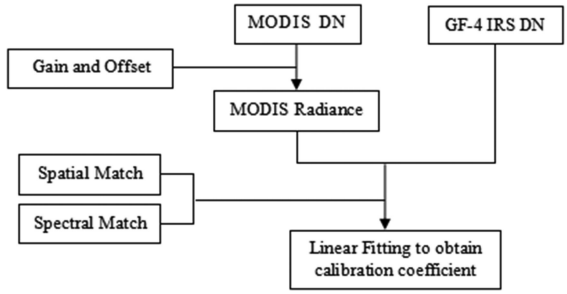

Fig. 2. Flowchart of the cross-calibration process.

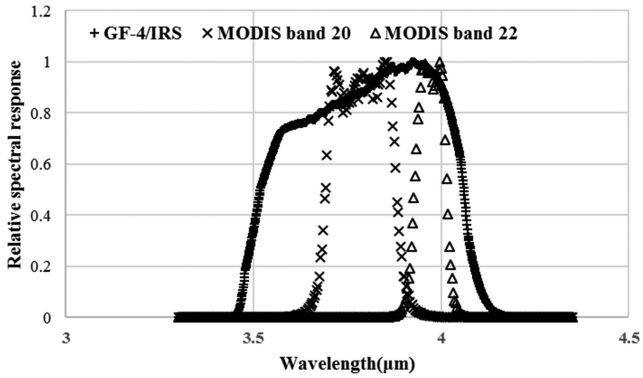

Fig. 3. Spectral response function of GF-4/IRS and MODIS band 20 and 22.

C. Spectral Match

Due to the spectral characteristics (e.g., the central wavelength (CW), bandwidth, and spectral response function] of the reference remote sensor and the to-be-calibrated remote sensor are generally different, spectral match must be carried out before calculating the calibration coefficients. In other words, it is necessary to eliminate the radiometric calibration error caused by the inconsistent spectral characteristics between corresponding bands. Spectral response function of GF-4/IRS and MODIS band 20 and 22 are plotted in Fig. 3. The x-axis represents the wavelength with the unit micrometer, and y-axis represents the relative spectral response which is unitless with the value range from 0 to 1. It is clearly shown that spectral response function is quite different between GF-4/IRS and a single band 20 or band 22. GF-4/IRS is a wide wavelength range band which covers the spectral range of both MODIS band 20 and 22, two narrow

TABLE II
SPECTRAL CHARACTERISTICS OF GF-4/IRS AND MODIS BAND 20 AND 22

Sensor	Band	Wavelength range (μm)	CW (μm)
GF-4/IRS	IRS	3.50-4.10	3.80
Terra/MODIS	Band 20	3.66-3.84	3.75
	Band 22	3.93-3.99	3.97

wavelength range bands. The detailed spectral characteristics of GF-4/IRS and MODIS band 20 and band 22 are given in Table II.

So far, the commonly used spectral methods for cross-calibration are ray matching method [19]–[21] and radiation transfer model method [22], [23]. The radiation transmission model method fully considers the radiometric difference between two sensors at various conditions, and can obtain a more accurate calibration coefficient. However, the radiation transfer model method requires more atmospheric parameters and *in situ* real-time measured data. The basis of the ray matching method is the single-band method, i.e., matching measurement of one un-calibrated band to that of another well-calibrated band. The advantage of the single-band method is that the calibration process is simple and calibration coefficient obtained is relatively reliable, especially for long-term time series. However, the single-band method does not take into account the spectral difference between two sensors, so that the calibration accuracy is not as good as radiation transfer model method.

In this article, based on the single-band method, we proposed the dual-band method to take the spectral difference between two sensors into account. In the dual-band method, we use three different approaches to calculate the weighting factor according to spectral response function.

1) Single-Band Method: The theory of single-band method is to calibrate the GF-4/IRS with one single MODIS band by ignoring spectral characteristic difference between bands. After spatial match, the valid calibration points are extracted from image pairs. Then the calibration coefficients are calculated by a linear fitting between GF-4/IRS DN and MODIS apparent radiance by using

$$L^i_{\mathrm{MOD}} = a \times \mathrm{DN}_{\mathrm{IRS}} + b \tag{1}$$

where $\mathrm{DN}_{\mathrm{IRS}}$ is the DN of GF-4/IRS at the test site. a and b are two critical coefficient parameters, i.e., gain and offset, to be obtained for GF-4/IRS. L^i_{MOD} is apparent radiance of MODIS band 20 or band 22, and can be calculated by

$$L^i_{\mathrm{MOD}} = \mathrm{gain}_i \times \left(\mathrm{DN}^i_{\mathrm{MOD}} - \mathrm{offset}_i\right) \tag{2}$$

where $\mathrm{DN}^i_{\mathrm{MOD}}$ and L^i_{MOD} represents digital number and apparent radiance of MODIS band i, respectively, while gain_i and offset_i are well-calibrated coefficient parameters of MODIS band i, and can be abstracted from MODIS science data set.

2) Dual-Band Method: Since the wavelength ranges of both MODIS band 20 and 22 are located within spectrum range of GF-4/IRS, the dual-band method is proposed to calibrate GF-4/IRS by treating two MODIS bands as reference band jointly. The difference between the single-band method and the dual-band method is that L_{MOD} is the measurement combination of band 20 and band 22, which is calculated by (3).

$$L_{\mathrm{MOD}} = C_1 \times \mathrm{L}^{B20}_{\mathrm{MOD}} + C_2 \times L^{B22}_{\mathrm{MOD}} \tag{3}$$

where $L^{\mathrm{B20}}_{\mathrm{MOD}}$ and $L^{\mathrm{B22}}_{\mathrm{MOD}}$ represent the apparent radiance of MODIS in band 20 and band 22 and are calculated by (2), respectively. $C1$ and $C2$ are the weight factors for two MODIS bands used in the dual-band method. For analysis purpose, we applied three approaches to compute weight factors for spectral match, including mean value approach, intersection value approach, and CW distance approach.

a) Mean Value Approach: The mean value approach is the simplest way to combine measurements of MODIS in band 20 and in band 22, by assuming two bands has the same contribution in final MODIS apparent radiance. Thus, the weigh factors $C1$ and $C2$ are both set to 0.5, and (3) is transformed to the following expression

$$L_{\mathrm{MOD}} = 0.5 \times L^{B20}_{\mathrm{MOD}} + 0.5 \times L^{B22}_{\mathrm{MOD}}. \tag{4}$$

b) Intersection Value Approach: Because the spectral response function of MODIS band 20 and 22 are not identical and allocated equally in two sides within GF-4/IRS spectrum segment, the calibration coefficients accuracy may increase if we treat two weight factors $C1$ and $C2$ unequally. From the spectral response function diagram, it is clear that the CW of MODIS band 20 and band 22 intersect with the spectral response function of GF-4/IRS at the intersection points. If we use $qB20$ and $qB22$ to stand for two corresponding values in y-axis, two weight factors $C1$ and $C2$ are calculated by formulas $C1 = qB20/(qB20 + qB22)$ and $C2 = qB22/(qB20 + qB22)$, respectively. Finally, $qB20$ and $qB22$ are equal to 0.4771 and 0.5229, respectively.

c) CW Distance Approach: From the Table II, the CW of MODIS band 20 is closer to the CW of GF-4/IRS than that of MODIS band 22. If the response combination of MODIS band 20 and band 22 is used to replace GF-4/IRS response, the response contribution from band 20 may larger than that of band 22.Therefore, the center wavelength distance approach is applied to calculate the weight factors by formulas $C1 = d2/(d1 + d2)$ and $C2 = d1/(d1 + d2)$ where $d1$ and $d2$ are the absolute values of the CW difference between reference bands and GF-4/IRS, with the value of 0.9372 and 0.0628, respectively.

IV. RESULT ANALYSIS AND DISCUSSION

A. Cross-Calibration Results

After spatial match, the spatial resolutions of image pairs are all scaled to 1000 m. According to the linear fitting method, all of the matching points extracted from three image pairs given in Table I are put together to obtain the cross-calibration coefficients with five schemes including single-band method using MODIS band 20, single-band method using MODIS band 22, dual-band method with the mean value approach, dual-band method with the intersection value approach, and dual-band method with the CW distance approach. The detailed results with five schemes are plotted in Fig. 4. The cross-calibration results of the article and the official calibration coefficients are given in Table III.

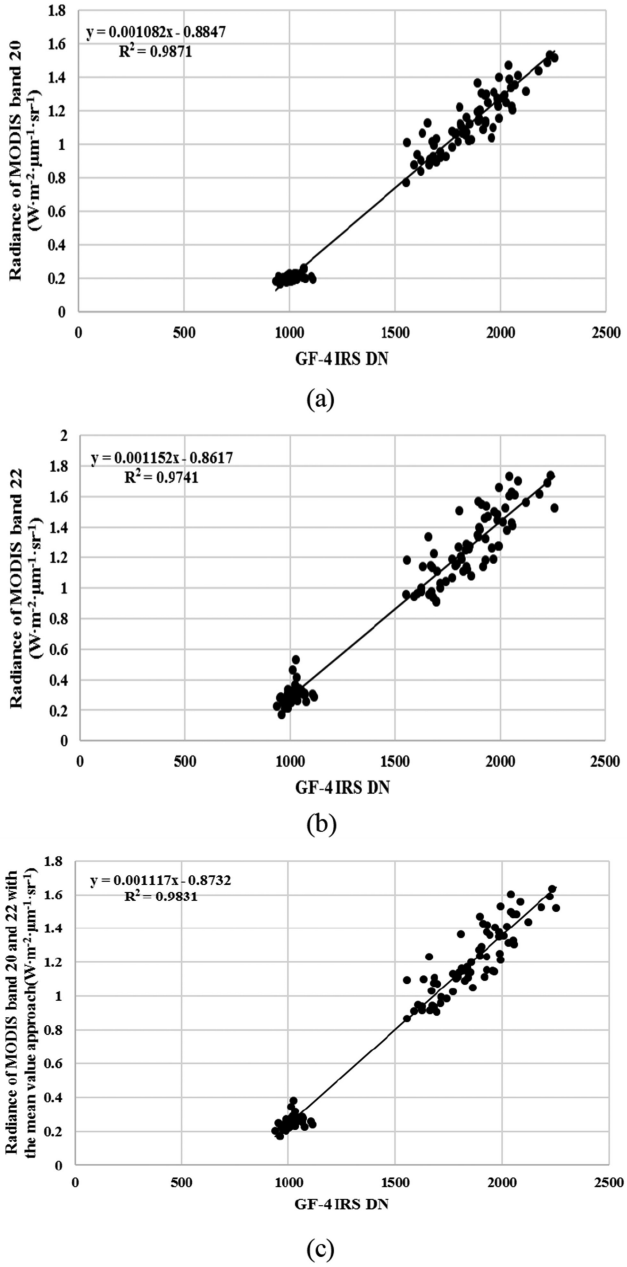

Fig. 4. Linear fitting results using five schemes. (a) Single-band method using MODIS band 20. (b) Single-band method using MODIS band 22. (c) Dual-band method with the mean value approach.

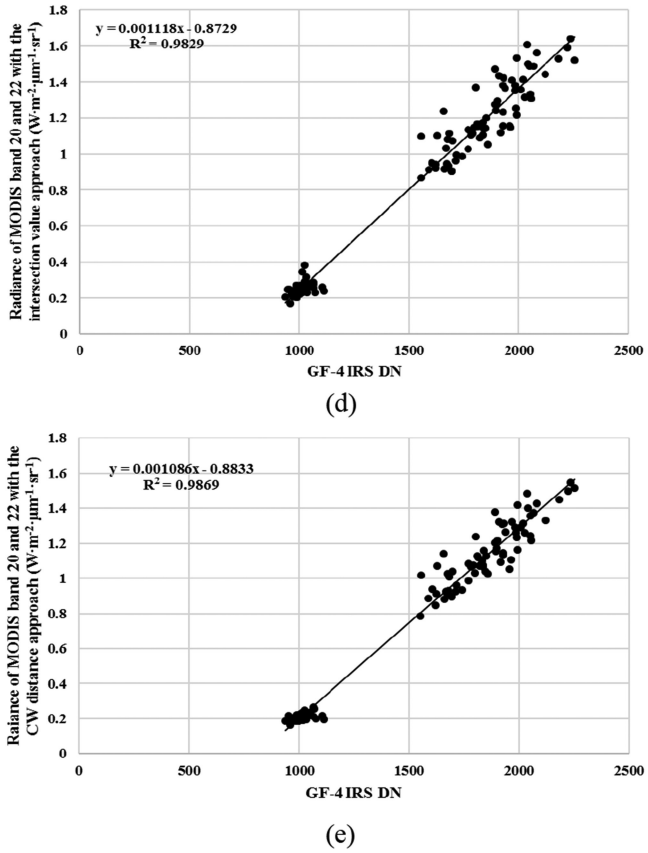

Fig. 4. *(Continued.)* Linear fitting results using five schemes. (d) Dual-band method with the inter-section value approach. (e) Dual-band method with the CW distance approach.

TABLE III
CROSS-CALIBRATION RESULTS USING FIVE SCHEMES AND THE OFFICIAL CALIBRATION COEFFICIENTS OF GF-4/IRS SENSOR

Scheme	Gain	Offset
(a)	0.001082	-0.8847
(b)	0.001152	-0.8617
(c)	0.001117	-0.8732
(d)	0.001118	-0.8729
(e)	0.001086	-0.8833
Official Calibration Coefficients	0.001107	-0.8786

B. Validation With the Official Calibration Coefficients

The official calibration coefficients, published in 2016 by the China centre for resources satellite data and application, with the site calibration method at Qinghai Lake are treated as the reference information, which has a sufficiently high accuracy to validate the cross-calibration result [16], [18], [24], [25].

Since the calibration coefficients are consist of gain and offset, the apparent radiance is treated as the investigated targets. Thus, the next step is to extract the valid validation points. In our validation process, integrating the negative offset of cross-calibration results and the official calibration coefficients, the DN range of typical surface features and the possible nonlinear response effects of GF-4/IRS sensor, the homogeneous surfaces satisfying the following two restrictive conditions are treated as the valid validation points. The CV of the sliding window (5×5pixels) in the original GF-4/IRS image is calculated. If the CV is lower than 3%, the corresponding homogeneous surface is treated as the candidate validation points. The range of the average DN value of the sliding window is from 820 to 3500.

According to the above filter condition, the valid validation points are extracted from five images to validate the calibration accuracy. The relative errors of the apparent radiance calculated with our cross-calibration results and the official calibration

TABLE IV
INFORMATION OF VALIDATION IMAGES AND THE STATISTICAL RESULTS

Date	Area	DN Range	Scheme	Mean error	Standard deviation
2016.05.11	Hai Nan	839-1994	(a)	-7.310%	0.0065
			(b)	14.312%	0.0132
			(c)	3.501%	0.0033
			(d)	3.804%	0.0036
			(e)	-6.058%	0.0054
2016.05.11	Tai Lake	824-2010	(a)	-7.308%	0.0108
			(b)	14.308%	0.0219
			(c)	3.500%	0.0056
			(d)	3.803%	0.0060
			(e)	-6.057%	0.0089
2016.05.30	Ordos	825-2699	(a)	-5.258%	0.1246
			(b)	10.148%	0.2527
			(c)	2.445%	0.0641
			(d)	2.662%	0.0693
			(e)	-4.367%	0.1026
2016.05.10	Bohai Sea	828-2285	(a)	-9.183%	0.1441
			(b)	18.109%	0.2923
			(c)	4.463%	0.0741
			(d)	4.845%	0.0802
			(e)	-7.600%	0.1187
2016.05.14	Korea Strait	821-2218	(a)	-9.121%	0.0412
			(b)	18.334%	0.1068
			(c)	4.431%	0.0212
			(d)	4.811%	0.0229
			(e)	-7.549%	0.0339

coefficients respectively are obtained. The relative error is defined as the value of "the apparent radiance calculated with the cross-calibration results / the apparent radiance calculated with the official calibration coefficients – 1." The information of validation images and the statistical results including the mean error and standard deviation are given in Table IV. Fig. 5 shows the corresponding relative error distribution.

According to Fig. 5 and Table IV, it can be found that the mean values of the scheme (c) in the five validation images are the minimum, approximately 3.668% and that of the scheme (b) in the five validation images are the maximum, approximately 15.042%. Meanwhile, the standard deviation of the scheme (c) in the five validation images are the minimum, approximately 0.0336, and that of the scheme (b) are the maximum, approximately 0.1374. The smaller mean value and standard deviation mean the cross-calibration results are higher radiometric calibration consistency with the official calibration coefficients. So, it can be concluded that the scheme (c) is the more suitable for the cross-calibration of GF-4/IRS sensor.

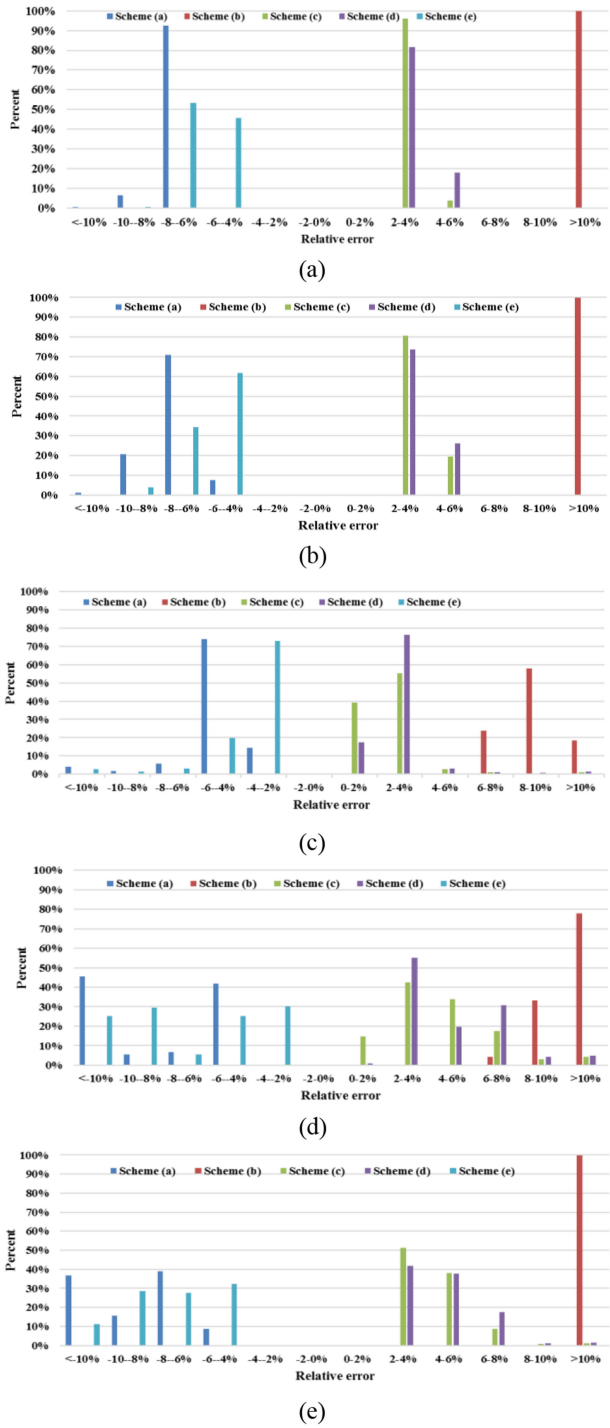

Fig. 5. Relative errors distribution based on five schemes in (a) Hai nan, (b) Tai Lake, (c) Ordos, (d) Bohai Sea, and (e) Korea Strait.

C. Stability of the Cross-Calibration Method

In the above cross-calibration process, all of the calibration points extracted from three image pairs are used to get the cross-calibration results given in Table III. In this part, we will discuss the stability of the proposed dual-band cross-calibration method with the mean value approach. Thus, each group of the calibration points extracted from single image pairs given in Table I is used to get the cross-calibration results given in Table V with the proposed dual-band cross-calibration method with the mean value approach. The relative errors of gain and that of offset between the cross-calibration results and the official calibration coefficients are also given in Table V. The relative error of gain is defined as the value of "the gain of the cross-calibration results / the gain of the official calibration coefficients – 1." The relative error of offset is defined as the value of "the offset of

TABLE V
STABILITY ANALYSIS RESULTS OF THE PROPOSED DUAL-BAND CROSS-CALIBRATION METHOD WITH THE MEAN VALUE APPROACH

Date	Gain	Offset	The relative error of gain	The relative error of offset
2016.05.10	0.001169	-0.9154	5.601%	4.188%
2016.05.11	0.001082	-0.8329	-2.258%	-5.201%
2016.05.14	0.001064	-0.8291	-3.884%	-5.634%

TABLE VI
VALIDATION RESULTS USING THE NEW DN OF GF-4/IRS IMAGE

Date	Area	Mean error	Standard deviation
2016.05.11	Hai Nan	3.302%	0.0050
2016.05.11	Tai Lake	3.300%	0.0082
2016.05.30	Ordos	1.740%	0.0948
2016.05.10	BoHai Sea	4.726%	0.1096
2016.05.14	Korea Strait	4.679%	0.0314

the cross-calibration results / the offset of the official calibration coefficients – 1." Table V gives that the relative error of gain is lower than 5.601% and the relative error of offset is lower than 5.634%. It indicates that the proposed dual-band cross-calibration method with the mean value approach has a high stability, which can provide a suitable cross-calibration method for GF-4/IRS to implement the time-series cross-calibration of GF-4/IRS and detect radiometric degradation throughout the whole period of operation.

D. Influence of Geometric Matching Errors on the Cross-Calibration Results

In our cross-calibration process, it is very important to accurately extract the information of calibration points including DNs of GF-4/IRS images and the corresponding radiance of MODIS images based on the geometric position. However, the geometric matching errors of calibration image pairs will affect the cross-calibration accuracy. Therefore, the shifted sliding-window method is used [26]. The sliding window (5×5pixels) of the resampled GF-4/IRS image is shifted by one pixel (1000 m) to extract the new DN of GF-4/IRS image. Then the original apparent radiance of MODIS images and the new DNs of GF-4/IRS images over the calibration points are used to recalculate the new cross-calibration results with the proposed dual-band cross-calibration method with the mean value approach. The same validation images given in Table IV are used to validate the cross-calibration accuracy. The validation results using the new DN of GF-4/IRS image are given in Table VI. Compared with Table IV, it is found that the mean error is slightly reduced from 3.668% to 3.550%, but the standard deviation is slightly increased from 0.0336 to 0.0498, which illustrates the geometric matching errors of the calibration image pairs have very little impact on the cross-calibration accuracy in the article.

V. CONCLUSION

GF-4 satellite operates in a geostationary orbit, observing the Earth with very high temporal resolution. Both PMS and IRS cameras are calibrated with site calibration method once per year at this stage, and may be affected by unexpected change. Therefore, we selected MODIS as the reference sensor to perform cross-sensor radiometric calibration of GF-4/IRS because MODIS has the outstanding radiometric calibration accuracy. Since the spectral response function of MODIS band 20 and 22 are both located within the spectral response range of GF-4/IRS, the single-band method and the dual-band method are proposed to compensate the relative spectral responses differences in this article. Then, the results from three sets of data imaging over Qinghai Lake and Se Lincuo Lake test site are obtained and analyzed.

With the statistical analysis, spectral matching using the dual-band method with the mean value approach by integrating measurements of two MODIS bands has a good correlation and can provide the highest radiometric calibration consistency with the official calibration coefficients than other spectral matching methods. The mean value of the apparent radiance difference when using the dual-band method with the mean value approach to obtain the cross-calibration results is approximately 3.668%. Meanwhile, the proposed dual-band cross-calibration method with the mean value approach can obtain the stable cross-calibration results. Additionally, the analysis results indicate the geometric matching errors between GF-4/IRS and MODIS image pairs have very little impact on the cross-calibration accuracy in the article.

In the future, we will implement long time-series of cross-calibration of GF-4/IRS based on MODIS measurements and discuss the radiometric attenuation of GF-4/IRS sensor during the entire period of operation.

ACKNOWLEDGMENT

The GF-4 images at the Qinghai Lake and Se Lincuo test site used in this research are supported by the China Centre for Resources Satellite Data and Application.[1] The MODIS data were downloaded from the Level 1 and Atmosphere Archive and Distribution System.[2] The authors would also like to thank the anonymous reviewers.

REFERENCES

[1] W. Y. Liu, "GF-4 launches to end space mission in 12th five - Year Plan," *Aerosp.* China, no. 1, pp. 20, 2016.
[2] W. Den, "GF-4 satellite," *Satell. Appl.*, no. 1, pp. 93, 2016.
[3] W. P. Ma and M. L. Lian, "Technical characteristics of the staring camera on board GF-4 satellite," *Spacecraft Recovery Remote Sens.*, vol. 37, no. 4, pp. 26–31, 2016.
[4] P. M. Teillet, P. N. Slater, and Y. Ding, "Three methods for the absolute calibration of the NOAA AVHRR sensors In-flight," *Remote Sens. Environ.*, vol. 31, pp. 105–120, 1990.
[5] F. Cabot, O. Hagolle, and P. Henry, "Relative and multitemporal calibration of AVHRR. SeaWiFS, and vegetation using POLDER characterization of desert sites," in *Proc. IEEE Int. Geosc. Remote Sens. Symp.*, 2000, vol. 1, pp. 2188–2190.
[6] G. Chander *et al.*, "Applications of spectral band adjustment factors (SBAF) for cross-calibration," *IEEE Trans. Geosci. Remote Sens.*, vol. 51, no. 3, pp. 1267–1281, 2013.
[7] K. J. Thome, F. B. Stuart, and W. Wisniewski, "Cross comparison of EO-1 sensors and other earth resources sensors to landsat-7 ETM+ using railroad valley playa," *IEEE Trans. Geosci. Remote Sens.*, vol. 41, no. 6, pp. 1180–1188, 2015.

[1] [Online]. Available: http://www.cresda.com/CN/
[2] [Online]. Available: https://earthdata.nasa.gov/about/daacs/daac-laads

[8] C. C. Moeller *et al.*, "An overview of the earth observing system MODIS instrument and associated data systems performance," in *Proc. IEEE Int. Geosci. Remote Sens. Symp.*, 2002, vol. 2, pp. 1174–1176.
[9] Y. Xie, A. Wu, and X. Xiong, "Tracking long-term stability of aqua MODIS and AIRS at different scan angles," *Proc. SPIE*, vol. 7807, Aug. 2010, Art. no. 780718.
[10] A. Wu, Y. Xie, X. Xiong, and I. W. Chu, "Assess calibration consistency of MODIS and AVHRR thermal infrared bands using SNO observations corrected for atmospheric effects," *IEEE Geosci. Remote Sens. Lett.*, vol. 9, no. 3, pp. 487–491, May 2012.
[11] L. Liu, Q. Y. Fu, and T. T. Shi, "Multi point cross calibration and verification of HJ-1B thermal infrared channel using AIRS hyperspectral data," *Scientia Sinica (Technologica)*, vol. 45, no. 1, pp. 103–110, 2015.
[12] H. Y. Yang, J. G. Li, and L. Zhu, "Calibration and analysis of HJ-1B/IRS thermal infrared channel based on historical data," *Infrared Laser Eng.*, vol. 45, no. 3, pp. 55–59, 2016.
[13] L. Liu, X. F. Gu, and T. Yu, "Site calibration and validation of HJ-1B satellite thermal infrared channel in orbit," *Infrared Laser Eng.*, vol. 41, no. 5, pp. 1119–1125, 2012.
[14] Y. Zhang, Z. G. Rong, and M. Min, "Accuracy evaluation of radiometric calibration method for the thermal infrared channel of china's remote sensing satellite radiometric calibration field," *Adv. Earth Sci.*, vol. 31, no. 2, pp. 171–179, 2016.
[15] W. L. Barnes, X. Xiong, and V. V. Salomonson, "Status of terra MODIS and aqua MODIS," in *Proc. IEEE Int. Geosci. Remote Sens. Symp.,* 2002, vol. 2, pp. 970–972.
[16] J. Han *et al.*, "A novel radiometric cross-calibration of GF-6/WFV with MODIS at the dunhuang radiometric calibration site," *IEEE J. Sel. Topics Appl. Earth Observ. Remote Sens.*, vol. 14, pp. 1645–1653, Jan. 2021.
[17] S. B. Li, "Application of cubic convolution interpolation to digital map data based on matlab," *J. Geomatics*, vol. 36, no. 3, pp. 36–38, 2011.
[18] J. Han, Z. Tao, Y. Xie, Q. Liu and Y. Huang, "Radiometric cross-calibration of GF-4/PMS based on radiometric block adjustment," *IEEE Trans. Geosci. Remote Sens.*, vol. 59, no. 6, pp. 4522–4534, Jun. 2021.
[19] D. R. Doelling, L. Nguyen, and P. Minnis, "Calibration comparisons between SEVIRI, MODIS and GOES data," in *Proc. Meteorolog. Satell. Conf.*, 2004, vol. 2004, pp. 17–20.
[20] G. M. Jiang, "Cross-calibration of MSGI-SEVIRI infrared channels with Terra-MODIS channels," *Int. J. Remote Sens.,* vol. 30, no. 3, pp. 753–769, 2009.
[21] P. M. Teillet and J. L. Barker, "Radiometric Cross-calibration of the landsat-7 ETM+ and landsat-5 TM sensors based on tandem data sets," *Remote Sens. Environ.*, vol. 78, pp. 39–54, 2001.
[22] A. Asem, P. Y. Deschamps, and D. Ho, "Calibration of METEOSAT infrared radiometer using split window channels of NOAA AVHRR," *J. Atmospheric Ocean. Technol.,* vol. 4, no. 4, pp. 553–562, 1987.
[23] E. F. Vermote and N. Z. Saleous, "Calibration of NOAA16 AVHRR over a desert site using MODIS data," *Remote Sens. Environ.*, vol. 105, no. 3, pp. 214–220, 2006.
[24] H. Gao, X. Gu, T. Yu, Y. Sun, and Q. Liu, "Cross-calibration of GF-1 PMS sensor with landsat 8 OLI and terra MODIS," *IEEE Trans. Geosci. Remote Sens.*, vol. 54, no. 8, pp. 4847–4854, Aug. 2016.
[25] Q. Liu, T. Yu, and H. Gao, "Radiometric cross-calibration of GF-1 PMS sensor with a new BRDF model," *Remote Sens.*, vol. 11, no. 6, pp. 707, Mar. 2019.
[26] G. Chander, D. L. Helder, D. Aaron, N. Mishra, and A. K. Shrestha, "Assessment of spectral, misregistration, and spatial uncertainties inherent in the cross-calibration study," *IEEE Trans. Geosci. Remote Sens.*, vol. 51, no. 3, pp. 1282–1296, Mar. 2013.

Xiang Zhou received the B.S. degree in cartography and geographic information system from Wuhan University, Wuhan, China, in 1999, the M.S. degree in computer sciences from Birmingham University, Birmingham, U.K., in 2004, and the Ph.D. degree in engineering from Beijing University of Technology, Beijing, China, in 2008.

He is currently a Professor with Aerospace Information Research Institute, CAS. His research interests include environment remote sensing, validation of remote sensing products and geospatial information science.

Duo Feng received the B.S. degree in 2021 from Nanjing University of Information Science and Technology, Nanjing, China, where he is currently working toward the M.S. degree in geography.

He has been working on the research of satellite sensor on-orbit radiometric calibration.

Yong Xie received the B.S. and M.S. degrees in physics from the Nanjing Normal University, Nanjing, China, in 2000 and 2004, respectively, and the Ph.D. degree in earth science and geoinformation system from George Mason University, Fairfax, VA, USA, in 2009.

He is currently a Professor with the School of Geographical Science, Nanjing University of Information Science and Technology, Nanjing, China. He has worked on the radiomimetic calibration and characterization of satellite remote sensor and science product validation with ground measurements.

Zui Tao was born in China in 1984. He received the B.S. degree from Henan University, Kaifeng, China, in 2005, the M.S. degree from Wuhan University, Wuhan, China, in 2008, and the Ph.D. degree from the Institute of Remote Sensing and Digital Earth, Chinese Academy of Sciences (CAS), Beijing, China, in 2012, all in cartography and geographic information system.

He is currently a Research Assistant with the Aerospace Information Research Institute, CAS. His research interests include validation of remote sensing product, ecological, and environmental remote sensing.

Tingting Lv received the B.S. and M.S. degrees in geology from Shandong Normal University, Jinan, China, in 2001 and 2004, respectively, and the Ph.D. degree in cartography and geographic information systems from the Institute of Geography and Natural Resources, Chinese Academy of Sciences (CAS) in 2010.

Since 2011, she has been a Research Assistant with the Aerospace Information Research Institute, CAS. Over the past few years, she has been involved in research on environmental monitoring based on RS and validation of remote sensing derived vegetation products.

Jin Wang received the M.S. degrees in hydro informatics from the China Institute of Water Resources and Hydropower Research, Beijing, China, in 2011.

She is currently an Assistant Researcher with the Aerospace Information Research Institute, Chinese Academy of Sciences, Beijing, China. She has been working on the validation of satellite remote sensing product, the acquisition and management of *in-situ* data, and the sharing of ground validation data from sites and experiments.